CHAPTER 2: LITERATURE REVIEW

2.1 Introduction to Biomaterials

The term biomaterials means, a nonviable material used in a medical device, intended to interact with biological systems. The next term that is essential in understanding the goal of biomaterial science is biocompatibility, which means the ability of a material to perform with an appropriate host response in a specific application (Williams, 1987). There have been trial and error attempts observed even before civilization such as the use of Nacre. In 1972, Mayan skulls which some of them dated more than 4000 years old with missing teeth was discovered to be replaced by nacre substitutes (Bobbio, 1972). Nacre is a natural composite consisting of 95–98 wt.% of calcium carbonate (aragonite, the 'ceramic' phase) and 2–5 wt.% of organic matter (fibrous proteins, polysaccharides).

The use of sutures to close large wound can be traced back thousands of years ago. Linen sutures and catgut were used by early Egyptians and Europeans in the middle age. The documentation on the use of sutures for medical application can be traced as early as 130–200 a.d. with the mention of gold wire ligatures by Galen of Pergamo. Phillips Physick, a Professor of Surgery from University of Pennsylvania reported little reaction with the usage of lead wires sutures in 1816 (Ratner, 2004). The surgical use of silver wire was already well known in the treatment of gynecological problems.

2.1.1 Polymer Based Biomaterials

Polyurethanes and polytetrafluoroethylene (Teflon) are polymer based materials discovered in the 1930's by Otto Bayer (Bayer, 1947) and Roy Plunkett (Garrett, 1962) respectively but only applied as biomaterials in the 1950s and 1960s. Polyurethanes were the first class of polymers to exhibit rubber elasticity without covalent cross-

linking (Seymour & Kauffman, 1992) used specifically for heart valves (Akutsu et al., 1959). Teflon was tested and found to be suitable material as synthetic vascular graft in the late 1960s (Feliciano et al., 1985; Ratner, 2004). Poly(2-hydroxyethyl methacrylate) (pHEMA) is a breakthrough for polymer based biomaterial used to produce soft contact lens in 1959 (Wichterle & Lim, 1960). UHMWPE (ultra-high molecular-weight polyethylene) is used untill today to produce prosthesis components known as total hip arthroplasty (THA) and total knee arthroplasty (TKA) which were introduced by Sir John Charnley around in the year 1960 (Charnley, 1961).

Polymer based biomaterials is easy to manufacture and versatile. However, various parameters have to be considered to acquire the desired characteristic which includes the choice0 of monomers, arrangement and length of polymer chain.

2.1.2 Metal Based Biomaterials

Metal alloy are usually used for components related to the skeletal system such as dental implants, joint and hard tissue replacement. The Romans, Chinese and Aztec used gold in dentistry more than 2000 years ago (Ratner, 2004). In the 19^{th} century iron, gold, lead, and porcelain were used either to replace teeth as artificial roots or as a coating for a replanted or transplanted tooth (Sullivan, 2001). Study has found gold, aluminum, and stellite are inert materials while silver, zinc and lead easily underwent corrosion. Copper caused bone stimulation and corroded slowly but steel and iron definitely inhibited bone regeneration and underwent corrosion (Zierold, 1924). Study on titanium as biomaterial began since 1950s proved to have higher tendency than noncorrosive alloys to fuse together with the bone and has the high tensile strength of 760 MPa and Young's modulus of 110 GPa compared 70-150 MPa and 15-30 GPa, respectively for cortical bone (Dee et al., 2003). Titanium based biomaterials have

favorable strength-to-density ratio and the TiO_2 (titanium oxide) film provides superior corrosion resistance. In general, the optimized characteristics of metal alloy compared to pure metal such as improved corrosion resistance and wear properties are suitable for biomedical applications (Katti, 2004; Binyamin et al., 2006).

2.2 Bioceramics

Bioceramics is an important subset of biomaterials. Bioceramics is generally separated into three families which are bioinert, bioactive and biodegradable with their respective mechanical properties shown in Table 2.1 and Table 2.2 respectively.

Table 2.1: Ceramics Used in Biomedical Application (Dee et al., 2003)

Ceramic	Chemical Formula	Comment
Alumina Zirconia	Al_2O_3 ZrO_2	Bioinert
Bioglass Hydroxyapatite (sintered at high temperature)	$Na_2OCaOP_2O_3$-SiO $Ca_{10}(PO_4)_6(OH)_2$	Bioactive
Hydroxyapatite (sintered at low temperature) Tricalcium phosphate	$Ca_{10}(PO_4)_6(OH)_2$ $Ca_3(PO_4)_2$	Biodegradable

Table 2.2 : Mechanical Properties of Different Ceramics (Chevalier & Gremillard., 2009)

Material	Fracture Toughness (K_{IC}, MPam$^{1/2}$)	4-Point Bending Strength (MPa)	Vickers hardness (Hv)
Alumina	4.2	400-600	1800-2000
Zirconia	5.4	1000	1200-1300
Hydroxyapatite	0.9	50-60	500
Tricalcium phosphate	1.3	50-60	900

Bioinert ceramic refers to material such as alumina and zirconia that do not induce any immunologic host reactions. However a fibrous capsule which isolate the bioinert ceramic material from the body is formed (Dorozkhin, 2010). The structure and mechanical properties of the bioinert ceramic is retained after implantation (Binyamin et al., 2006).

Bioactive ceramic refers to materials such as bioglass and hydroxyapatite sintered at high temperature that form bonds with living tissue which promote formation of apatite layer resulting with a strong bond between the tissue and the bioactive ceramic (Cao & Hench, 1996). Other bioactive bioceramic such as bioactive glasses are able to promote direct bone-implant adhesion without fibrous soft tissue interlayer but unable to be used as loaded devices (Dee et al., 2003).

Biodegradable ceramic refers to materials such as hydroxyapatite sintered at low temperature and calcium phosphate that degrade (by hydrolytic breakdown) in the body while they are being replaced by regenerating natural tissue. This newly formed tissue then grows into any surface irregularities which may not have direct interface the biodeagradable ceramic material (Jayaswal et al., 2010). Among biodegradable polymers, poly (lactic acid), poly (glycolic acid), and their copolymers have been widely used. Biodegradable polymers are used for sutures, controlled drug delivery, tissue engineering, and fracture fixation (Dee et al., 2003). These materials degrade into smaller fragments as well as monomers, such as lactic acid, that can be eliminated by normal metabolic processes of the body.

2.2.1 Aluminum Oxide

The first application of aluminum oxide (Al_2O_3) or alumina as biomaterial can be traced back to 1930 when Rock applied for the first patent (Rock, 1933). However it took more than 30 years until Sandhaus proposed and patented an alumina material for hip joints known as Degussit AL 23 in 1965 which can be considered as the great-grandmother of today's high tech ceramics (Sandhaus, 1965).

Alumina was introduced for orthopedic bearings, load bearing hip prostheses and dental implants in the 1970s due to its excellent biocompatibility, chemical inertness, high strength, good wear and corrosion resistance (Doremus, 1992). Alumina is a hard material with Vickers Hardness of 2000 Hv and high Young's Modulus of 380 GPa which is nearly double of stainless steel (Nizard et al., 2005). It is highly resistant to corrosion, abrasion, and contains hydrophilic property which allows better wettability of the surface to reduce wear progression. The reasons for the excellent wear and friction behavior of Al_2O_3 are associated with the surface energy and surface smoothness of this ceramic. However, alumina has lower fracture toughness value at approximately 4.5 $MPam^{1/2}$ when compared to human bone with fracture toughness of 2 $MPam^{1/2}$ to 10 $MPam^{1/2}$ making it brittle (Murugan & Ramakrishna, 2005) which is reflected in many reports on fracture rates due to their intrinsic brittleness (Campbell et al., 2004).

Biocompatibility test had shown that alumina is safe and has corrosion resistance with a low friction coefficient (Zeng, 2008). The bending strength of Al_2O_3 had increased over the last 40 years by improving metallurgical properties which included finer grain size and higher purity (Capello et al., 2005). Hot Isostatic Pressing (HIP) (Nizard et al., 2005) improved alumina manufacturing process. The HIPed alumina hip prosthesis has

reduced residual stresses within grain particles, reduced grain size and improved density. The evolution of Al_2O_3 main properties over the time are shown in Table 2.3.

Table 2.3: Progression of alumina (Al_2O_3) mechanical properties in the last four decades (Zeng, 2008; Masson, 2009)

Properties	**1970s (1st Generation)**	**1980s (2nd Generation)**	**1990s (3rd Generation)**
Mean grain size (µm)	<7	<3.2	1.5
Vickers hardness (Hv)	1800	1900	2000
4-point bending strength (MPa)	>400	>450	>500
Density (g/cm^3)	3.86	3.94	3.96

2.2.2 Zirconia

Zirconia ceramics are commonly used in orthopedic implant materials since the mid-1980s because it offers superior corrosion and scratch resistance relative to metals and better resistance against brittle fracture than alumina (Clarke et al., 2003). Surgical implant-grade zirconia is usually stabilized with either yttria (ASTM, 1998) or magnesia (ASTM, 2010b). Yttria-tetragonal zirconia polycrystals (Y-TZP) is mostly used than magnesia-stabilized zirconia (Mg-PSZ) in orthopaedic application because Y-TZP is nearly 100% tetragonal microstructure, which allows for a smaller grain size and greater hardness than Mg-PSZ. Furthermore, Y-TZP is easier to fabricate than Mg-PSZ, requiring relatively low sintering temperature of 1400 to 1550°C compared to 1800°C for Mg-PSZ (Piconi & Maccauro, 1999).

Y-TZP became a popular alternative to alumina and titanium for hip replacement (Manicone et al., 2007). The substantially higher fracture toughness of zirconia (6 to 15 $MPam^{1/2}$) is the consequence of increased crack propagation resistance (Denry & Kelly,

2008). New implant designs were possible with Y-TZP resulting in examples like the Y-TZP femoral heads and development of Y-TZP knees (Roy et al., 2007). The main application of zirconia ceramics is in Total Hip Replcement (THR) ball heads (Thamaraiselvi & Rajeswari, 2004). Approximately 600,000 zirconia femoral heads were used for clinical implantation since 1990 worldwide (Chevalier & Gremillard, 2009) and approximately 500,000 total hip and knee joint replacements were performed annually in the United States and Europe (Crowninshield et al., 2006).

However there is a downside discovered as Y-TZP is metastable at room temperature and can suffer accelerated spontaneous tetragonal-to-monoclinic phase transformation in the presence of water or water vapor (Chevalier, et al., 1999), a phenomenon known as hydrothermal ageing. The phase transformation induces weakening and surface roughening (Haraguchi et al., 2001) which increase the risk of wear-induced grain pullout (Deville et al., 2005). This low temperature hydrothermal degradation result in property degradation (Teoh, 2000; Chevalier, 2006; Borchers et al., 2010) and the viability of Y-TZP as a bearing surface (Santos et al., 2004).

2.2.3 Hydroxyapatite

Hydroxyapative (HA) is more commonly used as partial or full replacement parts for the human skeletal system such as dental implants because of it biocompatible and osteoconductive which makes it compatible with the bone (Ben-Nissan, 2003, Xin et al., 2005). Bioceramic is also chemically stable with high melting point, low in both thermal and electrical conductivity (Wang & Hon, 1999). However hydroxyapatite bioceramic has relatively poor fracture toughness about 1 $MPam^{1/2}$ when compared to bone fracture toughness which is between 2 to 12 $MPam^{1/2}$ (Hench, 1991). The clinical use of sintered HA is one of the remarkable successes of bioceramics.

One of the first papers that reports on this material for biomedical application was regarding hot-pressed hydroxyapatite powder into useful shapes for biological experimentation (Levitt et al., 1969). Similarities between the X-Ray diffraction patterns of bone material and HA was discovered in 1920 (Best et al., 2008) which means HA has similar components like the minerals in bones and teeth (Doremus, 1992). The osteoconductive property in HA promotes bone tissue growth (Sprio et al., 2009). In addition, hydroxyapatite also has been used as a coating on metallic orthopedic and dental implants to promote their fixation in bone. In these cases, the underlying metal carries the load, whereas the surrounding bone strongly bonds to hydroxyapatite. Delamination of the ceramic layer from the metal surface, however, can create serious problems and lead to implant failure (Dee et al., 2003).

The weak mechanical properties such as low fracture toughness (0.6-1MPa $m^{1/2}$) limit the scope of clinical application (Suchanek et al., 1998) and only applicable for nonload-bearing applications such as repair of bone defects, tooth root substitutes, filling of periodontal pockets, cystic cavities, coatings on metallic implants and spinal fusion (Bogdanovicience et al., 2006; Wang & Shaw, 2010). Hydroxyapatite is also used as filler for bone defects and as an implant in load-free anatomic sites (for example, nasal septal bone and middle ear) (Dee et al., 2003).

2.3 Introduction to Forsterite Bioceramic

Forsterite is a crystalline magnesium silicate with the chemical formula of Mg_2SiO4, named after the German scientist Johann Forster, in the magnesia–silica system which belongs to the group of olivine with orthorhombic structure (Saberi, et al., 2009; McDonnell et al., 2002). Forsterite is widely used in the electronics, communication and refractory applications. Forsterite ceramics are used as a dielectric material for high-

frequency circuits such as submillimetric-wave applications because of their low dielectric loss (ε = 6-7) with respect to extremely high-frequency electromagnetic waves (Tavangarian & Emadi, 2011a; Ohsato et al., 2004). The low electrical conductivity, low thermal expansion, good chemical stability and excellent insulation properties even at high temperatures make forsterite an ideal substrate material for electronic applications and tunable laser (Jing et al., 2009; Tavangarian & Emadi, 2010c; Tavangarian & Emadi, 2011). Forsterite is also widely used as refractory in the field of steel making and casting or ladle metallurgy due to its high melting point of 1890°C (Mustafa et al., 2002). Forsterite is an important material for solid oxide fuel cells (SOFC) applications since its linear thermal expansion coefficient perfectly matches the other cell components and it exhibits high stability in fuel cell environments (Kosanovic et al., 2005).

A variety of biocompatible graft materials have been used as substitute parts of hard tissue in the past decades (Scheer & Boyne, 1987; Piatteli et al., 1997). The development of bioceramics has provided promising alternatives in replacing damaged skeletal system. Forsterite (Mg_2SiO_4) and enstatite ($MgSiO_3$) are important materials in the magnesia-silica system. Enstatite has been reported as a new machinable biomaterial, and might be used in dental and orthopedic prostheses (Althoff et al., 1982; Goeuriota et al., 1998; Ni, et al., 2007). Enstatite ceramics possesses good mechanical properties but there are three different polymorphs that make enstatite unstable.

Therefore, parameters of the fabrication process including temperature, pressure and internal stress in grains should be strictly controlled. The destruction effect of phase transformation is caused by the difference in volumes of the grains. The intrinsic stress resulting from the volume changes lead to the loss of mechanical properties (Lee &

Heuer, 1987; Dubois et al., 1999; Mielcarek et al., 2004). Forsterite was found to possess similar fracture toughness to enstatite with K_{IC} = 2.4 MPam$^{1/2}$ which is higher than hydroxyapatite with K_{IC} = 1.0 MPam$^{1/2}$ (Chevalier & Gremillard, 2009). *In vitro* study showed significant osteoblasts adhesion, spreading and growing on the surface of forsterite ceramic indicating good biocompatibility which might be suitable for hard tissue repair (Ni et al., 2007).

2.4 Forsterite Phase Analysis

Forsterite consists of the the Mg^{2+} cation and SiO_4^{4-} anion in a molar ratio of 2:1 (Iishi, 1978). Within the SiO_4^{4-} anion, each oxygen atom is bonded to the central silicon atom by a single covalent bond. The four oxygen atoms need to stay far from each other to reduce the repulsive force between them because of the partial negative charge resulting from the covalent bond between the oxygen atom and silicon atom. The arrangement of the atoms results in the form of tetrahedral shape (Hazen, 1976; Downing et al., 2013).

The purity and reactivity of the prepared forsterite powder strongly depends on the firing temperature (Ando et al., 2007; Sano et al., 2006). The calcination temperatures for forming phase-pure forsterite have been reported to be around 800°C by co-precipitation (Yamaguchi et al., 1976), polymer precursor (Saberi et al., 2007) and citrate–nitrate routes (Saberi et al., 2009), above 1000°C by heterogeneous sol–gel method (Shiono et al., 1999), 1000°C to 1200°C using mechano chemical activation method (Fathi & Kharaziha, 2008b; Tavangarian et al., 2010; Tavangarian & Emadi, 2010d) and 1100°C to 1400°C by solid-state reactions between MgO and SiO_2 (Mitchell et al. 1998a).

The presence of water also has a profound effect on the original melting point of 1890°C which increases with pressure under anhydrous conditions but decreases with

pressure under water-saturated conditions. For example, at a pressure of 30 kbar the melting point of the anhydrous form has increased to approximately 2030°C, while the melting point of forsterite under water-saturated conditions at the same pressure has decreased to 1400°C (Deer et al. 1992). Forsterite undergoes a phase transition into wadsleyite $(Mg,Fe^{2+})_2(SiO_4)$ at high pressure of 14 GPa to 15 GPa which is similar to the condition at the transition zone of the Earth's upper mantle (Presnall, 1995; Kerschhofer et al., 1996). The definition of relationship between the phase compositions, microstructure and mechanical properties is used to determine the application range of this material as shown in Figure 2.1.

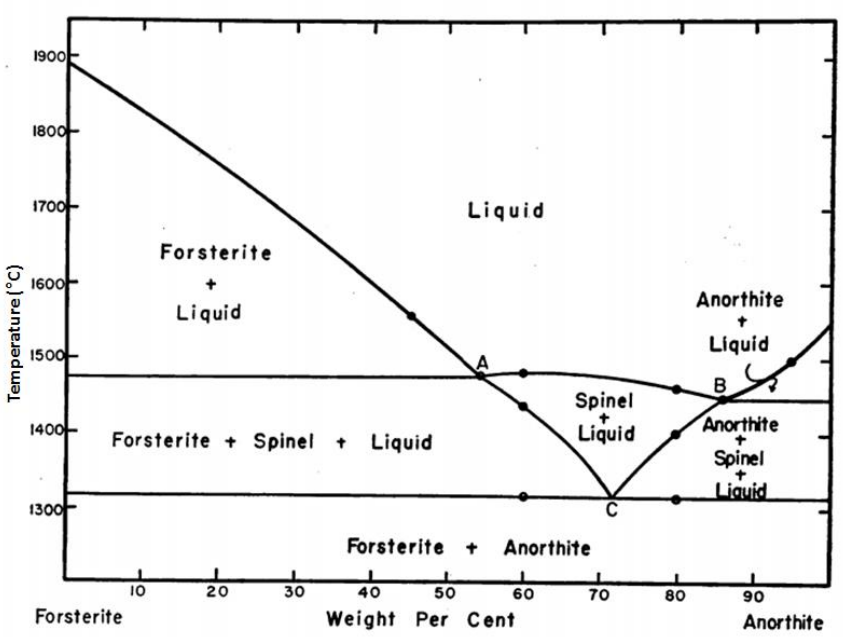

Figure 2.1: Equilibrium diagram for the join forsterite-anorthite (Osborn et al., 1952)

2.5 Synthesis of Forsterite Powder

There are several techniques used to synthesize forsterite powder which require different starting precursors and methodology. The starting precursors are mixed according to the stoichiometric ratio for Mg and Si as 2 to 1 respectively. The

commonly used synthesis methods include conventional solid-state reaction using high energy milling, citrate nitrate route and the sol-gel method.

2.5.1 Sol Gel Method

The main advantages of sol-gel method include the ability to produce homogeneous powders of a complex composition, lowering the temperature of synthesis, and controlling the morphology and phase composition (Vlasov & Krainova, 1988). There are several variants of the sol-gel process which depend on the kind of initial materials (solutions of metal salts, soluble hydroxides, alkoxides and salt solutions combined with organic polymers), the type of the medium (water, ammonia solution) and the mechanism of gel formation (Afonina et al., 2005).

The properties of material are determined by its composition and the method of gel production. Forsterite can be synthesized from the monophase and two phase sol. The starting precursors of magnesium nitrate hexahydrate, ($Mg(NO_3)_2 .6H_2O$) and tetra ethyl ortho silicate (TEOS) are used in the alkoxide method to form monophase forsterite (Afonina et al., 2005; Sanosh et al., 2010). For two phase sol, the common starting precursors used are magnesium nitrate hexahydrate, ($Mg(NO_3)_2 .6H_2O$) and colloidal silica (SiO_2) (Afonina et al., 2005). Polymer matrix and citrate nitrate methods using different types of starting precursors including citric acid and ammonia were used to form monophase sol at low temperature of 860°C (Saberi et al., 2009). Table 2.4 gives the synthesis parameters using sol gel method with different starting precursors to produce forsterite.

Sol gel method is effective to produce highly disperse powder by molecular mixing to high degree of homogeneity, reducing the crystallization temperature and prevent phase segregation during heat treatment (Tsai, 2002). However, nonuniform precipitation and

chemical inhomogeneity of gels occur due to the different hydrolysis rate between silicon and other alkoxides for multi component silicate system such as forsterite. This mismatch can cause higher crystalline temperature and formation of undesirable secondary phases (i.e. enstatite and magnesium oxide) which inhibit the formation of pure forsterite after heat treatment at 1200°C to 1300°C (Tsai, 2002). Furthermore, sol gel method requires longer processing time including drying and ageing of the gel to form forsterite poweder (Ni, et al., 2007; Kharaziha & Fathi, 2009;2010).

Table 2.4: Forsterite powder synthesis using sol gel method with different starting precursors ([1] Sanosh et al, 2010; [2]Saberi et al., 2009; [3] Kharaziha & Fathi, 2010;[4] Saberi et al., 2007; [5] Mitchell et al., 1998b; [6] Ni et al., 2007)

Starting Precursors	Heat Treatment Duration	Crystallite Size (nm)
$(Mg(NO_3)_2.6H_2O)$, TEOS	800°C for 30 minutes[1]	22
$(Mg(NO_3)_2.6H_2O)$, Colloidal SiO_2, ammonia solution, citric acid	860°C for 1 hour[2]	27-30
$(Mg(NO_3)_2.6H_2O)$, Colloidal SiO_2, sucrose, nitric acid, polyvinyl alcohol polymer (PVA)	800°C for 2 hours[3]	17-20
$(Mg(NO_3)_2.6H_2O)$, Colloidal SiO_2, sucrose, nitric acid, polyvinyl alcohol polymer (PVA)	800°C for 3 hours[4]	10-30
$Mg(OEt)_2$, 2-methoxyethanol, TEOS	1200°C for 1 hour[5]	10 nm
$(Mg(NO_3)_2.6H_2O)$, Colloidal SiO_2	1200°C for 3 hours[6]	-

2.5.2 Mechanical Activation

Solid state reaction which is also known as mechanical activation or high energy ball milling has been widely used for synthesizing nanocrystalline materials (Castro & Mitchell, 2002). The planetary ball mill owes its name to the planet-like movement of its vials. These are arranged on a rotating support disk, and a special drive mechanism

which cause them to rotate around their own axes. The centrifugal force produced by the vials rotating around their own axes and that produced by the rotating support disk both act on the vial contents, consisting of material to be ground and the grinding balls. Since the vials and the supporting disk rotate in opposite directions, the centrifugal forces alternately act in opposite directions. This causes the grinding balls to run down the inside of the vial (friction effect) followed by the material being ground. Grinding balls lift off and travel freely through the inner chamber of the vial and collide against the opposing inside wall (impact effect). This strong impact energy enhances the contact area and interaction of reactants resulting in particle size reduction which help to form the nano-size structure product with enhanced properties including high hardness and high strength compared to coarse-grain materials (Kiss et al., 2001). Table 2.5 shows forsterite powder synthesized by mechanical activation with different starting precursors and ball milling duration.

Table 2.5: Forsterite Powder Synthesized by Mechanical Activation
([1]Fathi & Kharaziha, 2008b; [2]Tavangarian & Emadi, 2010d; [3]Tavangarian & Emadi, 2010a; [4]Tavangarian et al., 2010; [5]Tavangarian & Emadi, 2009; [6]Fathi & Kharaziha, 2008a; [7&8]Tavangarian & Emadi, 2010b; [9&10]Tavangarian & Emadi, 2010c)

Starting precursors	**Ball milling duration**	**Heat treatment temperature**	**Heat treatment dwell time**	**Crystallite size (nm)**
$MgCO_3$, SiO_2, $(NH_4)_2SiF_6$	5 hours[1]	900°C	1 hour	18
$MgCO_3$, NH_4F, talc	5 hours[2]	1000°C	1 hour	53
$MgCO_3$, talc	5 hours[3]	1000°C	1 hour	40
$MgCO_3$, talc	10 hours[4]	1000°C	10 min	30
$MgCO_3$, talc	10 hours[5]	1000°C	1 hour	40
$MgCO_3$, SiO_2	10 hours[6]	1200°C	1 hour	30-57
$MgCO_3$(calcined), talc(calcined)	40 hours[7]	1000°C	1 hour	49
$MgCO_3$(calcined), talc(calcined)	40 hours[8]	1200°C	1 hour	63
$MgCO_3$, talc	10 hours[9]	1000°C	1 hour	40
MgO, talc	5 hours[10]	1000°C	1 hour	60

There are several different combination of starting precursors to form forsterite powder including magnesium carbonate ($MgCO_3$) and talc (Tavangarian & Emadi, 2009 & 2010a; Tavangarian et al., 2010). Fluorine ion and chlorine ion were found to enhance forsterite formation rate during mechanical activation process (Tavangarian & Emadi, 2010d & 2011). Forsterite powder was successfully formed after 5 hours of mechanical activation process with the addition of fluorine ion compared to 10 hours without the presence of fluorine ion (Fathi & Kharaziha, 2008b) because the additional element act as intermediate transition compounds (chondrodite, humite and clinohumite), that enhance the forsterite formation reaction (Tavangarian & Emadi, 2010d). Ammonium hexafluorosilicate ($(NH_4)_2SiF_6$) and Ammonium fluoride (NH_4F) are the compounds containing fluorine which act as catalyst (Tavangarian & Emadi, 2010d; Fathi & Kharaziha, 2008b & 2009a).

Longer ball milling time does not guarantee smaller crystallite size as shown in Table 2.5. However, it is proven that regardless of the type of starting precursors, forsterite could not be synthesized with ball milling duration less than 1 hour (Tavangarian & Emadi, 2009 & 2010a) and the increase in ball milling duration helps in reducing secondary phase to form pure forsterite (Tavangarian et al, 2010) as typically shown in Figure 2.2.

Pure forsterite was formed after ball milling for 10 hours followed by heat treatment at 1000°C for 1 hour using the $MgCO_3$ and talc combination (Tavangarian et al, 2010). The extended ball milling duration of 20 hours to 100 hours followed by heat treatment at 1000°C for 1 hour showed no significant effect on the structure and phase composition (Tavangarian & Emadi, 2009).

Figure 2.2: XRD traces of forsterite prepared by reacting $MgCO_3$ & talc after different mechanical activation duration & annealing at 1000°C for 1 hour (Tavangarian & Emadi, 2009)

In another study, MgO and enstatite peaks are still present after 5 hours mechanical activation for the $MgCO_3$ and talc combination (Tavangarian & Emadi, 2010c) as shown in Figure 2.3. Fast disappearance of MgO diffraction peaks observed in Figure 2.3 is the result of the milling effect on reaction rate. During mechanical activation process, magnesium carbonate is partially decomposed and crystallite sizes are reduced to nano scale. Decomposition of magnesium carbonate leads to the generation of CO_2 gas. Liberation of CO_2 gas which resulted in the formation of micro pores decreases grain sizes and increases the contact surface between grains and forsterite formation diffusion control process.

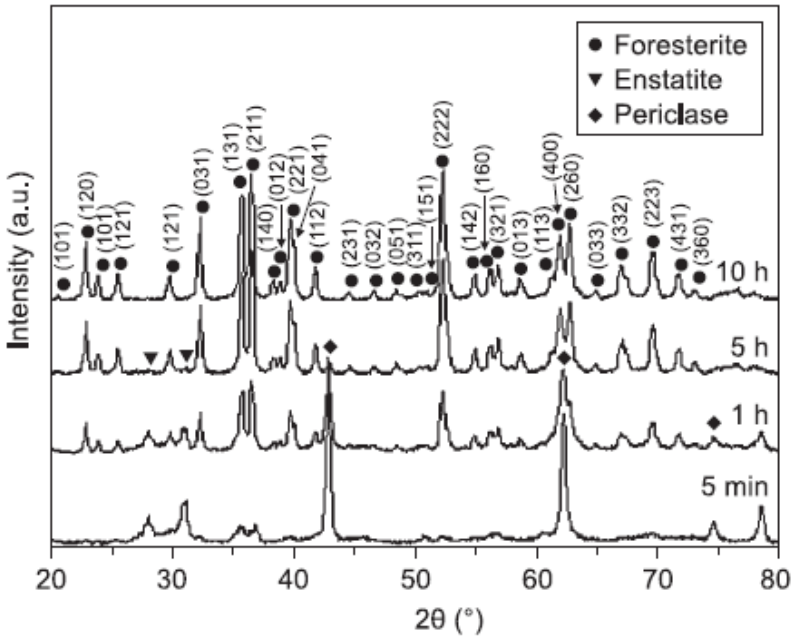

Figure 2.3: XRD traces of forsterite prepared by reacting $MgCO_3$ & talc after different mechanical activation duration & annealing at 1000°C for 1 hour (Tavangarian & Emadi, 2010c)

The combination of MgO and talc was found to react better than $MgCO_3$ with shorter ball milling duration (Tavangarian & Emadi, 2010c) of 5 hours. The absence of MgO and enstatite on XRD traces indicates that during mechanical activation, a homogeneous powder mixture was achieved. The result in Figure 2.4 indicates that some imperceptible $MgSiO_3$ must have remained in the sample for the stoichiometry ratio of 2:1 for Mg:Si in the forsterite. This situation is frequently encountered in the synthesis of forsterite. Even after heating up to 1540°C for 5 hours, which is close to the melting point of enstatite, $MgSiO_3$ and MgO had not completely reacted to form Mg_2SiO_4 (Douy, 2002). The common ball milling duration used for heat treatment profiles are 5 minutes, 1 hour, 5 hours and 10 hours (Tavangarian & Emadi, 2010a; Tavangarian et al, 2010).

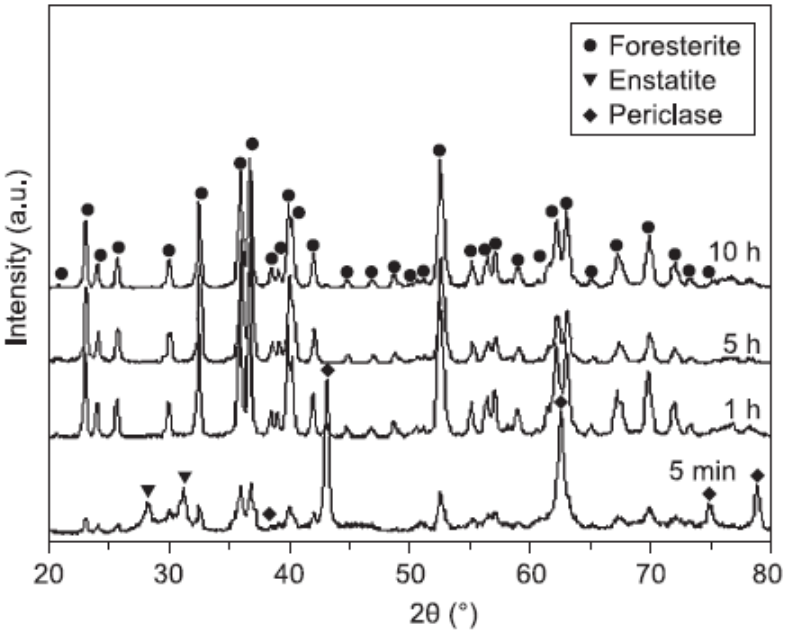

Figure 2.4: XRD traces forsterite prepared by reacting MgO & talc after different mechanical activation duration & annealing at 1000°C for 1 hour (Tavangarian & Emadi, 2010c)

Besides planetary ball milling, the conventional ball milling method is also commonly used for producing forsterite. A conventional ball mill consists of a rotating horizontal drum half-filled with choice of milling media having specific diameters (Castro & Mitchell, 2002). During the milling process, the media drop on the material particle that is being ground as the drum rotates. The rate of grinding increases with the speed of rotation. The centrifugal force acting on the milling balls exceeds the force of gravity and the milling balls are pinned to the wall of the drum at high speeds. The cascading motion move the milling balls along the drum's wall and rolling upon each other from the bulk's top to its base (Rosenkranz et al., 2011). The energy is transferred from the drum to the material particle at each collision resulting in finer size particles (Gavrilov et al., 1999). Pure forsterite powder was successfully synthesized by conventional ball milling for 10 hours using MgO and talc as starting precursors (Tan et al., 2015). Ball milling overcomes some problems associated with conventional blending methods such as thermal degradation due to excessive heating in the melting process, or the difficulty

in removing the polymer from the solvent if the solution method is used (Castro & Mitchell, 2002).

2.5.3 Other Synthesis Techniques

There are other forsterite powder synthesis techniques such as the aqueous route which involved mixing magnesium nitrate hexahydrate ($Mg(NO_3)_2.6H_2O$) to distilled water. Silicon tetrachloride ($SiCl_4$) was added and then heat treated at 1200°C for 24 hours to produce forsterite powder with crystallite size of 50 nm (Mitchell et al., 1999).

Another aqueous route used to synthesize forsterite powder was by directly hydrolyzing tetra ethyl ortho silicate (TEOS) into magnesium nitrate hexahydrate (Douy, 2002). The solution was sprayed through a 0.5 mm nozzle with compressed air in a parallel flow of air heated to 200°C. The collected powders were used for thermal analyses by initially heat treatment of 500°C for 1 h to completely decompose the nitrates. Further thermal treatment to 1200°C for 1 hour successfully form single phase forsterite powder which means $MgSiO_3$ had reacted with MgO as shown in Figure 2.5.

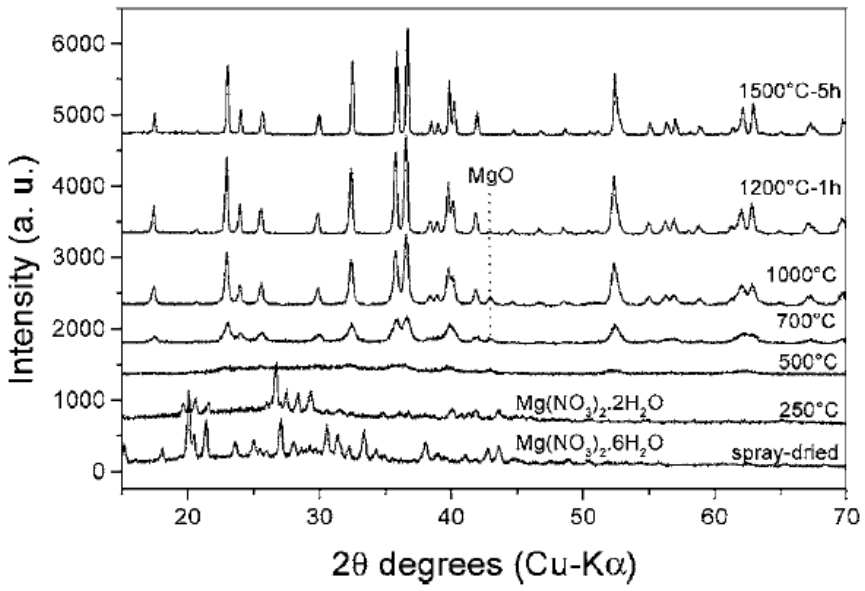

Figure 2.5: XRD traces of spray-dried precursor powder of Mg_2SiO_4 heated at different temperatures (Douy, 2002**)**

No other crystalline phase was detected after heat treatment at higher temperatures, up to 1500◦C. The same precursor solution was evaporated to dryness for comparison as shown in Figure 2.6.

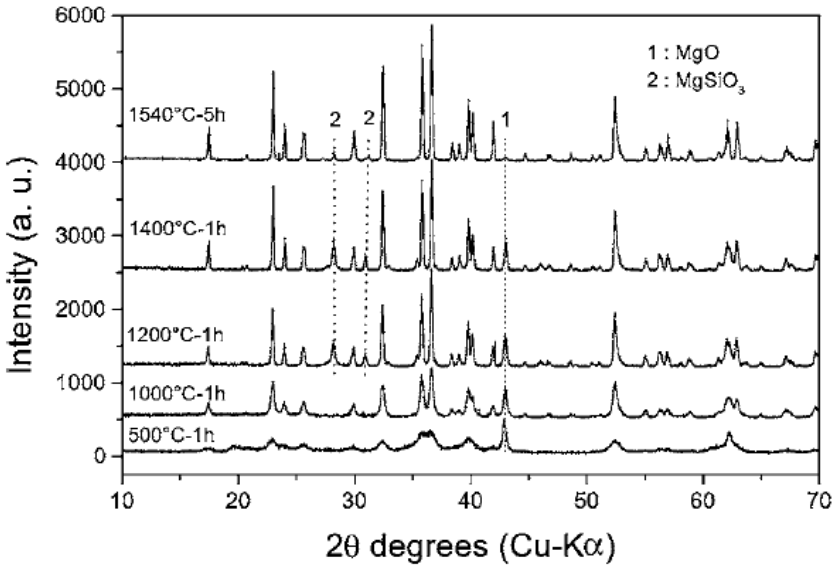

Figure 2.6: XRD traces of evaporated precursor powder of Mg_2SiO_4 heated to the indicated temperatures (Douy, 2002)

MgO peak was present at higher amount for the evaporated dried sampled (Figure 2.6) compared to the spray-dried sample (Figure 2.5). In Figure 2.6, Mg_2SiO_4 and MgO were observed after heat treatment at 1000°C. $MgSiO_3$, as protoenstatite (JCPDS file 11-273), appeared only at higher temperature while MgO was still present at 1400°C. MgO had not completely reacted together to form Mg_2SiO_4 even after heat treatment up to 1540°C which is the temperature close to the melting point of enstatite for 5 hours. The lack of reactivity between magnesium oxide and silicates indicates the precursor powders are not chemically homogeneous, and require higher thermal treatment temperature to obtain single phase forsterite. Therefore it is important to control the phase development for temperatures higher than 1000°C.

Forsterite pellet consist of forsterite powder and 3% kaolin using polyvinyl alcohol polymer as binder was sintered at 1450°C for 2 hours (Rani et al., 2014). The forsterite powder was synthesized via solid state reaction using magnesium oxide (MgO) and quartz (SiO_2). The addition of kaolin showed enhanced densification due to formation of cordierite ($(Mg,Fe)_2Al_3(Si_5AlO_{18})$) phase which melts at sintering temperature before forsterite by forming a low viscosity glassy phase.

Response surface methodology (RSM) using polyacrylamide gel method was used to optimize the densification of forsterite nanopowder (Hassanzadeh-Tabrizi, 2014). Magnesium nitrate hexahydrate (and tetra ethyl ortho-silicate (TEOS) were used as starting precursors. Forsterite powder was formed after heat treatment at 900°C for 3 hours and densification of 98.1% was obtained.

Ceramics synthesis is a complicated process which requires several numbers of steps and should be optimized for manufacturing feasibility without affecting properties. Minor physical or chemical defects can give severe effect on the ceramics properties. Suitable raw materials and processing conditions are very important factors to avoid mistakes that are irreversible during heat treatment and sintering processes. Therefore it is crucial to optimize the synthesis techniques to manufacture high purity fosterite powder which has good sinterability and superior mechanical properties.

2.6 Sinterability of Forsterite Ceramic

The study done so far revolves around the governing parameters which affects the purity and mechanical properties of forsterite powder such as the type of starting precursors used and synthesis methods which were discussed in sub-Chapter 2.5, subtitle 2.5. The elimination of secondary phases depends largely on the attributes of as-synthesized crystals resulting in superior forsterite mechanical properties (Kharaziha

and Fathi, 2010). The process of consolidation normally produces large-grained microstructures and consequently poor mechanical properties for standard pressureless sintering because it requires high temperature, slow heating rate and long holding time to achieve a dense body (Ni et al., 2007). Within the synthesis methods, there are varying factors that will influence the formation of forsterite powder including the effect of heat treatment and non heat treatment powder, the effect of sintering temperature and dwell time.

2.6.1 Heat Treatment Temperature

The heat treatment process enhances the formation of forsterite and optimizes the properties of the starting precursors mixed during the synthesis process. The heat treatment temperature that forms pure forsterite powder differs according to the starting precursors. For starting precursors of $MgCO_3$ and talc, XRD traces of magnesium carbonate pentahydrate ($MgCO_3.5H_2O$) was observed after ball milling for 5 minutes without heat treatment as shown in Figure 2.7. Broadening of XRD peaks and a significant decrease in the intensities was observed after 5 hours of ball milling. Subsequent increment in ball milling duration up to 100 hours as shown in Figure 2.7.

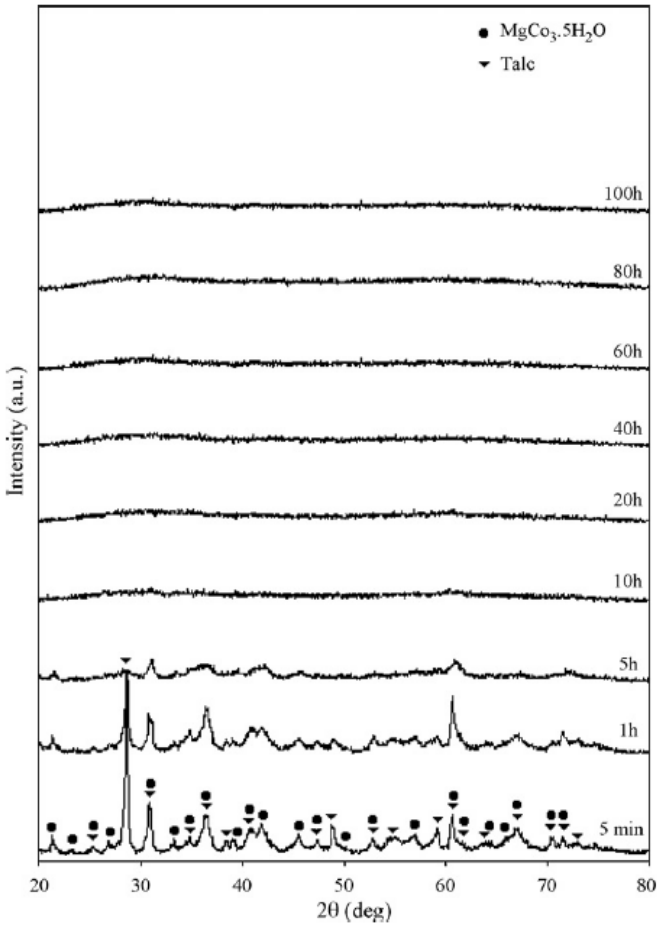

Figure 2.7: XRD traces forsterite prepared by reacting $MgCO_3$ & talc after different mechanical activation duration without heat treatment (Tavangarian & Emadi, 2009)

Figures 2.8 and 2.9 show the XRD traces of the forsterite ($MgCO_3$ & talc mixture) after heat treatment at 1000°C and 1200°C for 1 hour respectively. Pure forsterite could be formed after planetary ball milled for 5 hours and heat treatment at 1200°C for 1 hour (Tavangarian & Emadi, 2009 & 2010a) but 10 hours of planetary ball milled was required for heat treatment at 1000°C for 1 hour as shown in Figure 2.10. The reaction rate is higher at 1200°C than 1000°C but enstatite peak was present after prolonged planetary ball mill followed by heat treatment at 1200°C for 1 hour as shown in Figure 2.9.

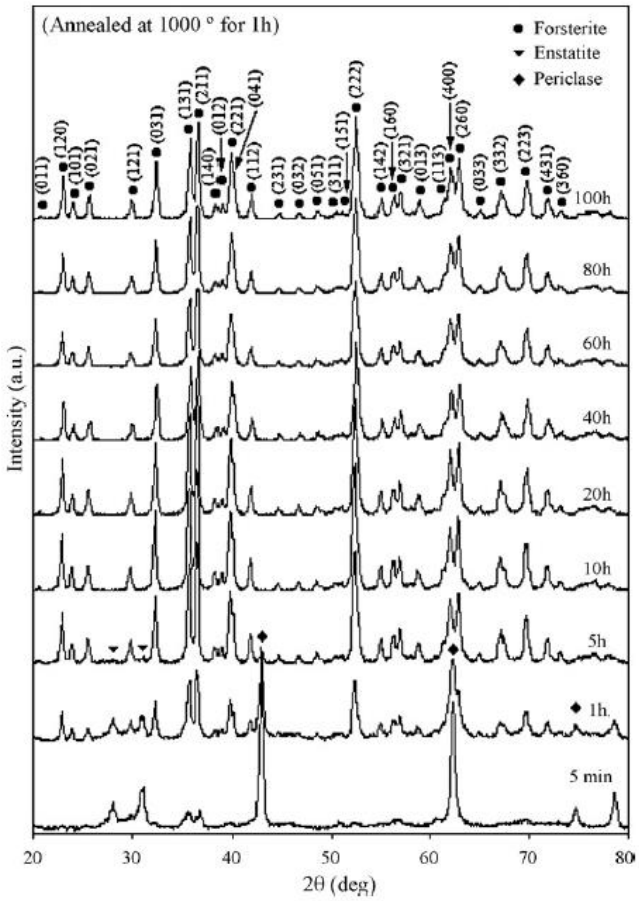

Figure 2.8: XRD traces of forsterite prepared by reacting $MgCO_3$ & talc after different mechanical activation duration & annealing at 1000°C for 1 hour (Tavangarian & Emadi, 2009)

The secondary phase, enstatite vanished after 40 hours and 60 hours planetary ball milling respectively. However, the XRD peaks of enstatite appeared again after 80 hour and 100 hours planetary ball milling because the free energy change the formation of Mg_2SiO_4 ($\Delta G_{1200°C}$ = −61.145 kJ/(mol K)) is more negative than that for $MgSiO_3$ ($\Delta G_{1200°C}$ = −40.542 kJ/(mol K)). Therefore the enstatite phase formed at 1200°C is thermodynamically metastable and forsterite is the more stable phase. The meta-stable enstatite phase is formed with increasing heat treatment temperature probably because of faster kinetics which appeared to be stable up to 1600°C (Kazakos et al, 1990). Planetary ball milling process can significantly enhance the kinetics of solid-state reactions (Suryanarayana, 2001).

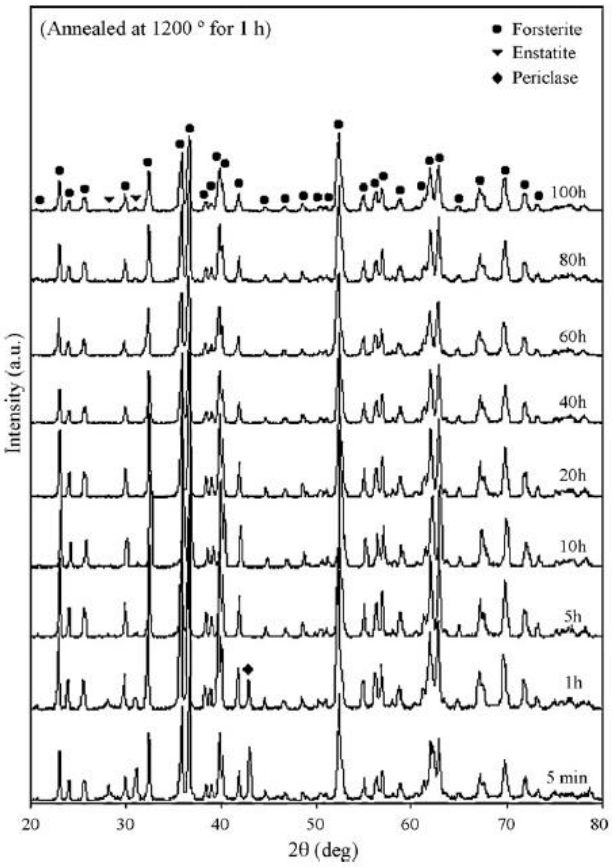

Figure 2.9: XRD traces of forsterite prepared by reacting $MgCO_3$ & talc after different mechanical activation duration & annealing at 1200°C for 1 hour (Tavangarian & Emadi, 2009)

The effect of higher heat treatment at various temperatures for 10 minutes is shown in Figures 2.10 and 2.11. Forsterite, magnesium oxide (MgO) and enstatite ($MgSiO_3$) could be fabricated by 5 hours mechanical activation with subsequent heat treatment at 1000 °C for 10 minutes as shown in Figure 2.10. The forsterite phase increased by increasing the ball milling time while the MgO and enstatite contents reduced after increasing heat treatment temperatures. However even after heat treatment at 1400°C for 10 minutes, $MgSiO_3$ and MgO were not completely reacted to form Mg_2SiO_4 (Tavangarian et al., 2010).

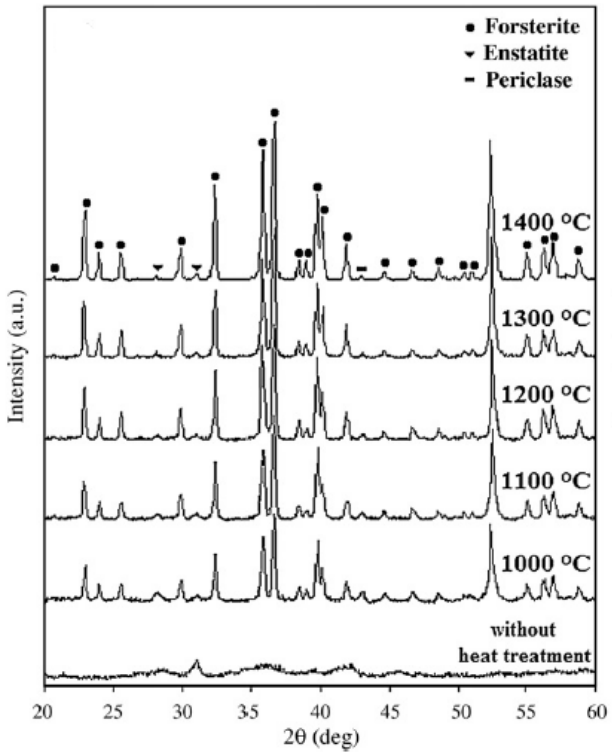

Figure 2.10: XRD traces of forsterite prepared by reacting $MgCO_3$ & talc after mechanical activation for 5 hours & heat treatment for 10 minutes (Tavangarian et al., 2010)

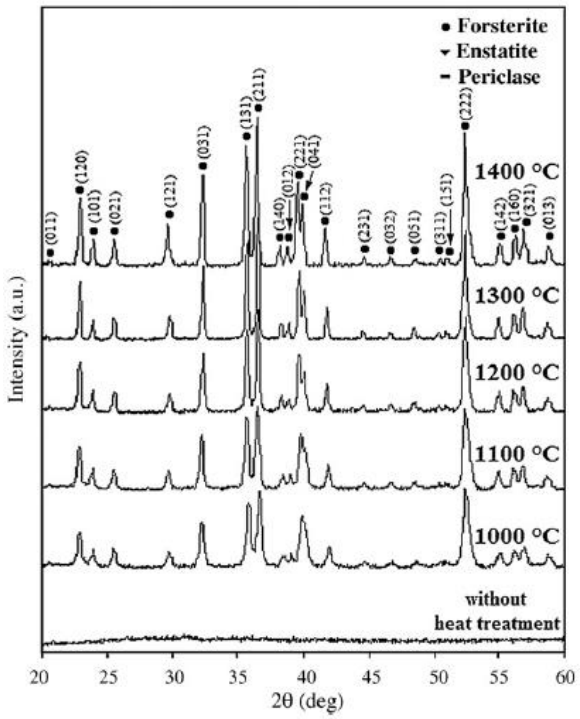

Figure 2.11: XRD traces of forsterite prepared by reacting $MgCO_3$ & talc after mechanical activation for 10 hours & heat treatment for 10 minutes (Tavangarian et al., 2010)

Figure 2.11 shows only forsterite phase could be observed after the sample was ball milled for 10 hours followed by heat treatment for 10 minutes at 1000°C, 1100°C, 1200°C, 1300°C and 1400°C. $MgCO_3$ particles got finer and partially decomposed during ball milling process, which indicates mechanical activation gradually changes the mixtures into amorphous state (Tavangarian & Emadi, 2010e). Mechanical activation increases the interface of the reacting phases which enhance the reaction kinetics during heat treatment process. $MgCO_3$ partially decomposes to MgO and CO_2 during mechanical activation (Kostic et al., 1997). The absence of MgO and $MgSiO_3$ in the 10 hours ball milled sample with subsequent heat treatment at 1000 °C for 10 min could be due to the amorphous state of these phases. Increasing the heat treatment temperature up to 1400°C for the sample with 10 hours ball milling had no significant effect on the structure and phase composition of the samples, although the peaks intensity increased and their widths decreased because of the internal strain recovery and the growth of crystallite size (Tavangarian & Emadi, 2009). The absence of MgO and $MgSiO_3$ on the XRD patterns indicates that homogeneous powder mixture was obtained during mechanical activation.

Figure 2.12 shows the XRD patterns after mechanical activation of magnesium oxide (MgO) and talc as starting precursors for various periods of time. Ball milling without heat treatment could not create amorphous structure and MgO peaks still persisted even after 10 hours of ball milling.

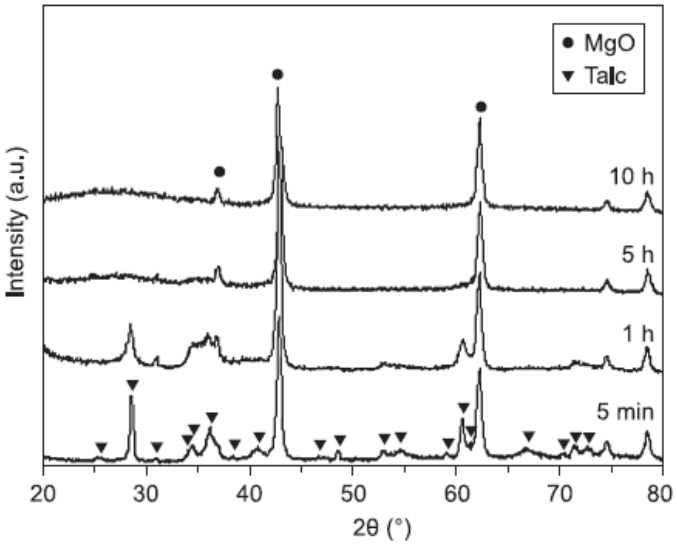

Figure 2.12: XRD traces of forsterite prepared by reacting MgO & talc after various mechanical activation duration without heat treatment (Tavangarian & Emadi, 2010c)

Pure forsterite could be formed after 5 hours planetary ball milling and heat treatment at 1000°C and 1200°C for 1 hour using MgO and talc (Tavangarian & Emadi, 2010c) as shown in Figure 2.13 and 2.14. MgO and enstatite disappeared after ball milling for 5 hours followed by heat treatment at 1000°C for 1 hour as shown in Figure 2.13. This formation of forsterite occurred through a diffusion control mechanism (Brindley & Hayami, 1965). MgO initially diffuses into the surface of the SiO_2 to form enstatite, and diffusion continues through this enstatite layer to form forsterite. This can be promoted by dynamically maintained high reaction interface areas as well as the short-circuit diffusion path provided by the large number of defects such as dislocations and grain boundaries induced during ball milling.

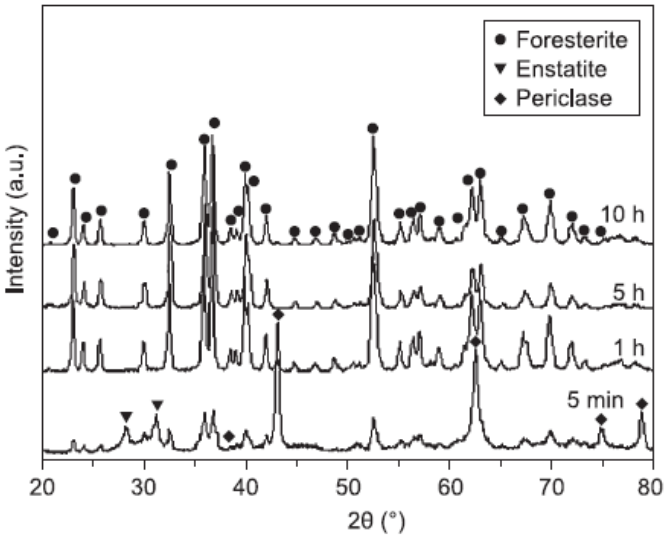

Figure 2.13: XRD traces of forsterite prepared by reacting MgO & talc after various mechanical activation duration and heat treatment at 1000°C for 1 hour (Tavangarian & Emadi, 2010c)

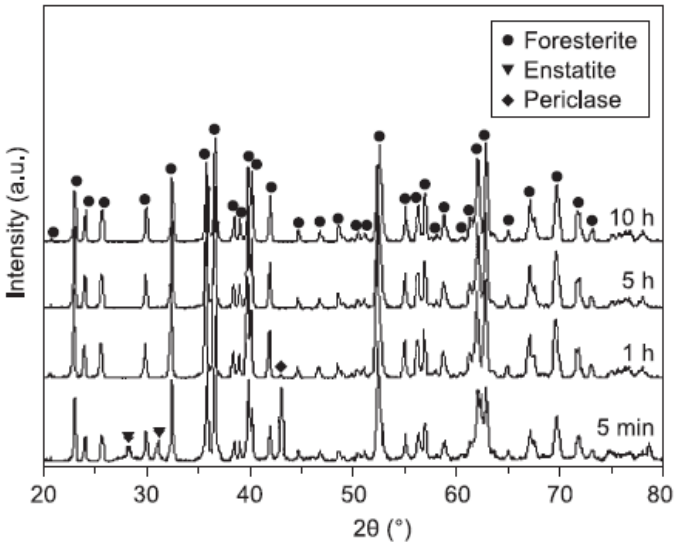

Figure 2.14: XRD traces of forsterite prepared by reacting MgO & talc after various mechanical activation duration and heat treatment at 1200°C for 1 hour (Tavangarian & Emadi, 2010c)

In Figure 2.14, pure forsterite phase was obtained after 5 hours ball milling while the magnesium oxide and enstatite contents reduced gradually as the ball milling duration increased followed by heat treatment at 1200°C for 1 hour. Further ball milling up to 10 hours had no significant effects on the structure or phase composition of the samples after subsequent heat treatment. The presence of MgO instead of $MgCO_3$ as starting

precursor showed that forsterite could be fabricated with lower ball milling duration followed by heat treatment process. This could be due to the absence of CO_2 which is the byproduct from the decomposition of magnesium carbonate, which caused the initial materials to be completely agglomerated after mechanical activation. Therefore, during mechanical activation, a homogeneous powder mixture was achieved and caused better reactivity between initial materials.

Investigation using longer ball milling duration up to 60 hours was performed without heat treatment (Tavangarian & Emadi, 2010a) and the result is shown in Figure 2.15.

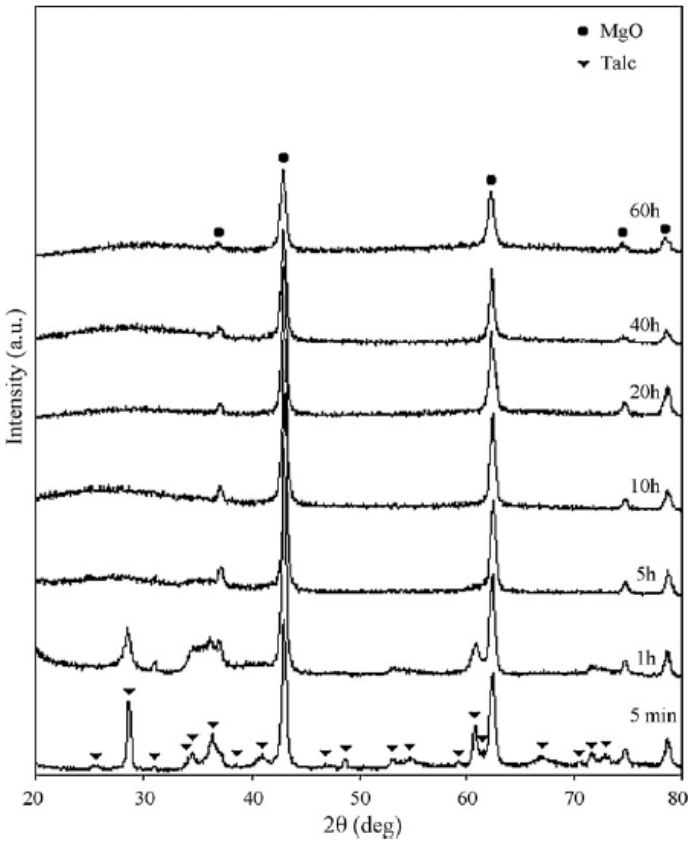

Figure 2.15: XRD traces of forsterite prepared by reacting MgO & talc after various mechanical activation duration without heat treatment (Tavangarian & Emadi, 2010)

The XRD patterns of starting precursors after 5 minutes of ball milling corresponded to those of talc (XRD JCPDS data file No. 13-0558) and MgO (XRD JCPDS data file No.

43-1022) phases. The talc peaks disappeared after 5 hours of mechanical activation because the ball milling process gradually drives talc into an amorphous state. But MgO peaks still persisted even after 60 hours of ball milling. Increasing the ball milling time up to 60 hours led to the broadening of XRD peaks and significant decrease in their intensity. This is the result of refinement in crystallite size and enhancement of the lattice strain. No new crystalline phase was observed in the XRD patterns. The effect of heat treatment at 1000°C and 1200°C on this mixture of MgO and talc is shown in Figure 2.16 and Figure 2.17.

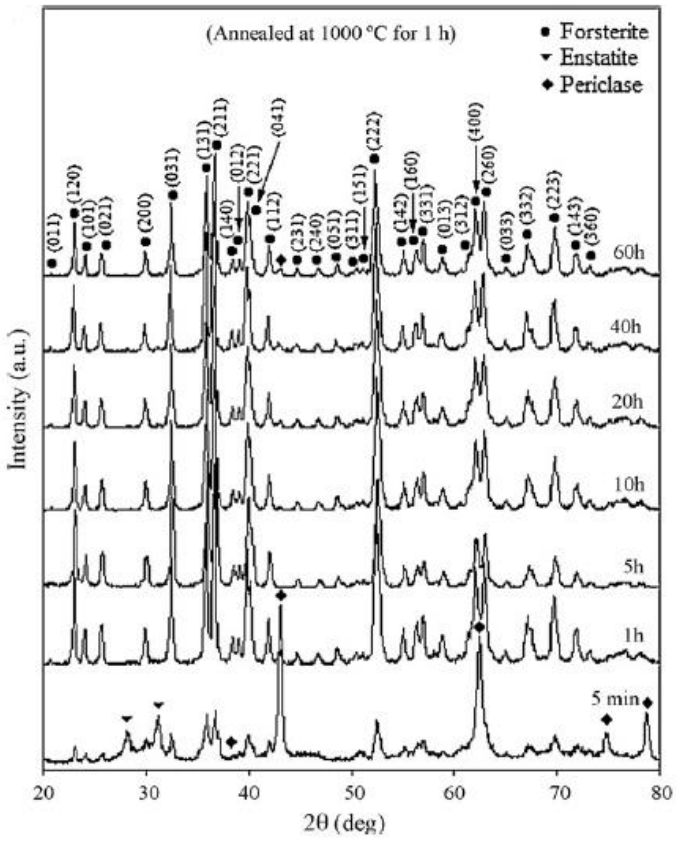

Figure 2.16: XRD traces of forsterite prepared by reacting MgO & talc after various mechanical activation duration & heat treatment at 1000°C for 1 hour (Tavangarian & Emadi, 2010a)

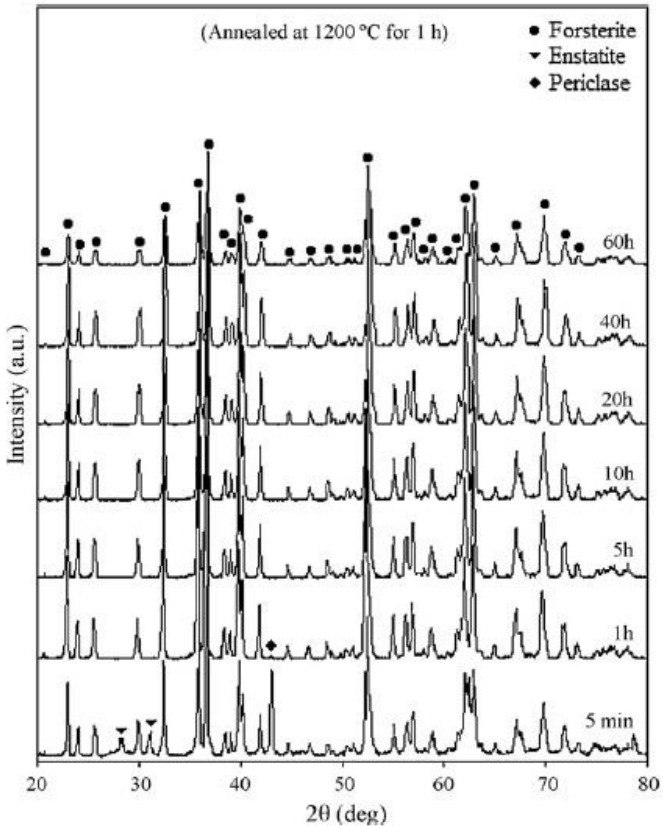

Figure 2.17: XRD traces of forsterite prepared by reacting MgO & talc after various mechanical activation duration & heat treatment at 1200°C for 1 hour (Tavangarian & Emadi, 2010a)

Talc peaks disappeared after 5 minutes of ball milling for both heat treatment temperatures 1000°C and 1200°C respectively for 1 hour as shown in Figure 2.18 and 2.19 because the talc has reacted with MgO to produce enstatite ($MgSiO_3$). This is evident with traces of enstatite (XRD JCPDS data file No. 11-0273) and forsterite (XRD JCPDS data file No. 34-0189). The magnesium oxide peaks which re-appeared after 10 hours of ball milling before heat treatment disappeared after heat treatment at 1000°C and 1200°C for 1 hour. This indicates that some imperceptible $MgSiO_3$ must have remained in the sample for the stoichiometry ratio of 2:1 for Mg:Si in the forsterite. The combination of ball milling and heat treatment is an improvement over previous studies where MgO had not completely reacted to form Mg_2SiO_4 even after heat treatment up to 1540°C for 5 hours, which is close to the melting point of enstatite (Douy, 2002). No significant effects on the structure or phase composition observed

after extended ball milling duration up to 60 hours. The results here indicate that heat treatment at 1200°C is more stable than 1000°C when MgO and talc were used as starting precursors.

2.6.2 Sintering Temperature and Dwell Time

The effect of sintering temperature and dwell time were investigated using forsterite powder that were prepared by sol–gel method using reagent-grade magnesium nitrate hexahydrate and colloidal SiO_2 as precursors with an initial MgO to SiO_2 molar ratio of 2. Heat treatment at 1200°C was applied for 3 hours to form the forsterite which was uniaxial pressed at 10 MPa to form a rectangular compact (45.5 mm x 8.0 mm x 3.5 mm) followed by cold isostatic pressing at 200 MPa. The green samples were subsequently sintered in air at temperatures ranging between1350°C to 1550°C with a heating rate of 2°C/min and then furnace cooled (Ni et al., 2007). The XRD traces of the sintered forsterite ceramic are shown in Figure 2.18.

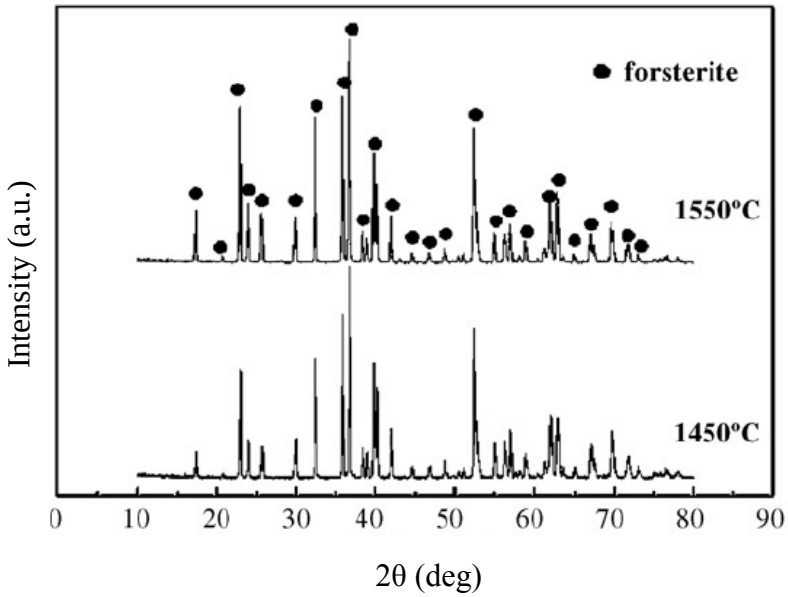

Figure 2.18: XRD traces of forsterite ceramic sintered at 1450°C and 1550°C for 8 hours (Ni et al., 2007)

The XRD traces in Figure 2.18 clearly showed only forsterite peaks were present when sintered at 1450°C and 1550°C for 8 hours respectively. There was no phase decomposition of the forsterite powder into unfavorable phases such as MgO and enstatite. This result is an improvement over previous findings where heat treatment did not have any apparent effect on the enstatite phase until heat treatment temperature reached 1600°C. Enstatite was detected only after heat treatment temperature at 1200°C (Kazakos et al., 1990). No other crystalline phase was detected for heat treatment up to 1300°C for 2 hours where prolonged heating lead to the formation of enstatite (Ban et al., 1999). The effect of various sintering temperatures on the relative density of forsterite is shown in Figures 2.19.

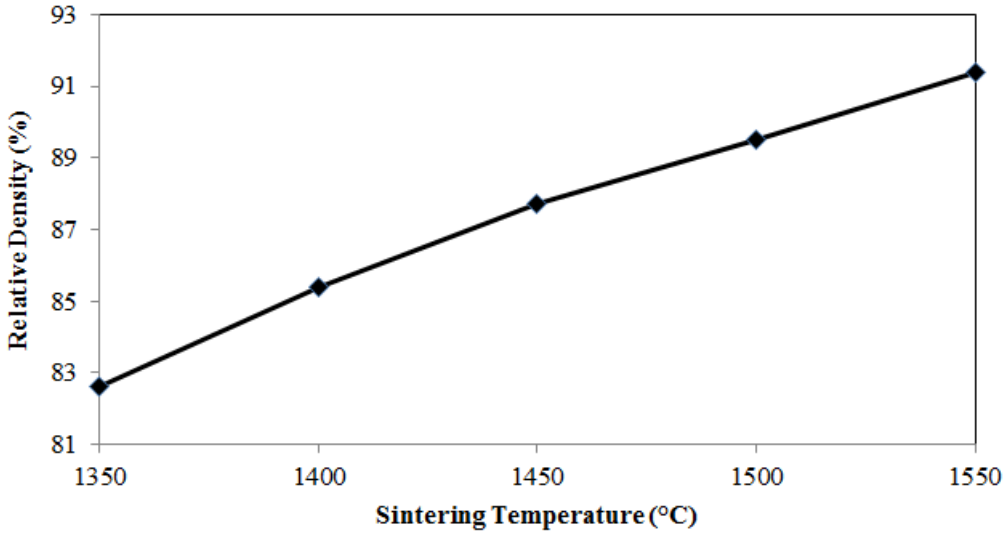

Figure 2.19: Effect of sintering temperature on relative density for sintered forsterite ceramic at various temperature for 8 hours (Ni et al., 2007)

The relative density increased linearly from 82.6% to 91.4% as the sintering temperature increased from 1350°C to 1550°C as shown in Figure 2.19. In addition, the mechanical strength of forsterite ceramics was enhanced with the increasing sintering temperature up to 1450°C. The bending strength and fracture toughness reached maximum values of 181 MPa and 2.3 $MPam^{1/2}$, respectively at 1450°C (Ni et al., 2007).

In general, the density and grain size of ceramics significantly affects the mechanical properties (Rice, 1996; Shi, 1999). High sintering temperatures often result in extreme grain coarsening. This was evident in the fractography, where the fracture surface of the forsterite ceramics sintered at 1450°C and 1550°C showed significant difference. Grain growth and densification occur simultaneously as long as the intergranular pores are eliminated through diffusion. Once a few grains start to grow abnormally fast by consuming small matrix grains surrounding them, pores get trapped within or between the excessively large grains and thus further densification becomes practically impossible. The specimen sintered at 1450°C had an average grain size of about 10 µm with sharp edged pores which were observed mainly between the grains as shown in Figure 2.20.

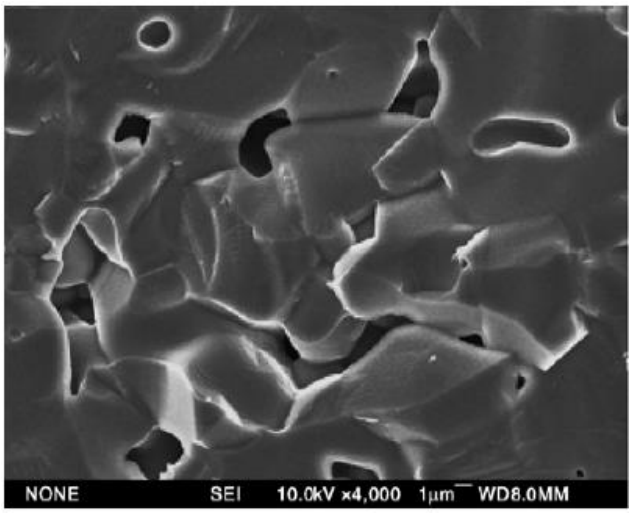

Figure 2.20: SEM monograph of forsterite ceramic fracture surface after sintering at 1450°C for 8 hours (Ni et al., 2007)

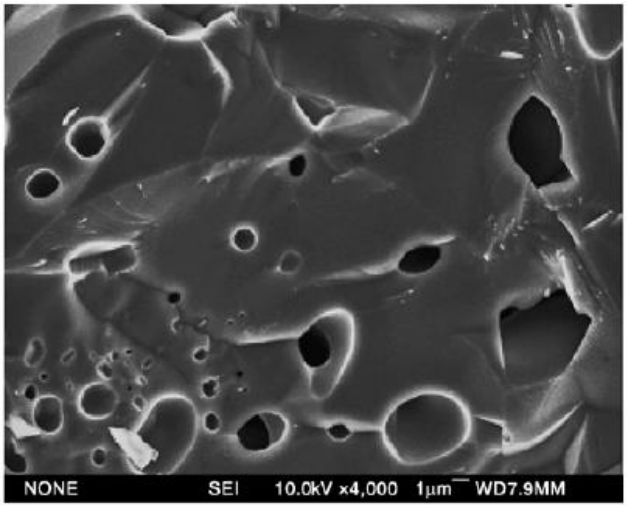

Figure 2.21: SEM monograph of forsterite ceramic fracture surface after sintering at 1550°C for 8 hours (Ni et al., 2007)

Further increase in sintering temperature up to 1550°C caused the pores to be trapped in the grains as a result of grain growth as shown in Figure 2.21 according to Ni et al., 2007. This phenomenon is the cause for the decreasing mechanical properties when the sintering temperature increased to 1550°C. Therefore the optimum sintering temperature for better mechanical properties was identified at 1450°C for 8 hours.

The effect of different dwell time was investigated by Ni et al., 2007 using forsterite ceramic sintered at 1450°C with heating rate of 2°C per minute. The sintering dwell time is an important factor which has an effect on the mechanical properties of the sintered fosterite ceramics. The relative density showed gradual increment from 86.6 % to 87.7 % as the sintering dwell time increased from 3 hours to 6 hours and sharp increase to 92.5 % for 8 hours dwell time. There was a linear increasing trend for bending strength with 152 MPa, 181 MPa and 213 MPa for sintering dwell time of 3 hours, 6 hours and 8 hours, respectively. Similarly, fracture toughness trend was also a linear one with 2.1 $MPam^{1/2}$, 2.3 $MPam^{1/2}$ and 2.4 $MPam^{1/2}$ being measured respectively. Overall, the experimental results showed that mechanical strength

increased linearly with increasing sintering dwell time which correlates with bulk density.

There was an investigation on the effect of sintering temperature on forsterite powder prepared by solid-state reaction, using magnesium oxide and talc as starting precursors (Tan et al. 2015). The mixed powders were then subjected to 2 minutes of high-frequency vibrations in an ultrasonic bath to ensure a homogenous mixing followed by 10 hours of ball milling to further refine the powder particles. This was followed by heat treatment at 1200°C for 2 hours. The prepared forsterite powder was uniaxial compacted at about 2.5 MPa to 3.0 MPa into round compacts. The green bodies were subsequently cold isostatically pressed at 200 MPa. The pellets were sintered via conventional pressureless sintering at temperatures ranging from 1200 to 1500°C for 2 hours with heating/cooling rate of 10°C/min and then furnace cooled to room temperature at 10°C/min.

The effect of sintering temperature on relative bulk density, fracture toughness and Vickers hardness are shown in Figures 2.22, 2.23 and 2.24 respectively.

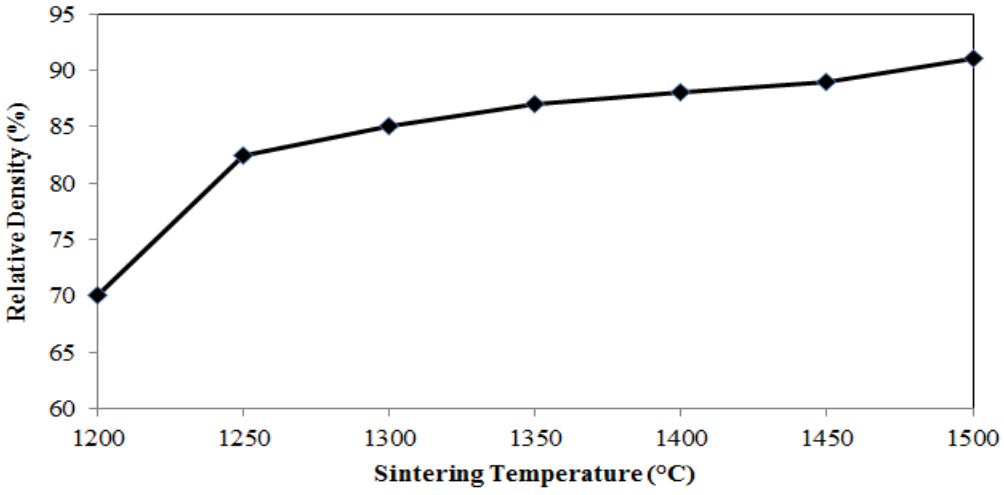

Figure 2.22: Effect of sintering temperature on relative density for sintered forsterite ceramic at various temperature for 2 hours (Tan et al., 2015)

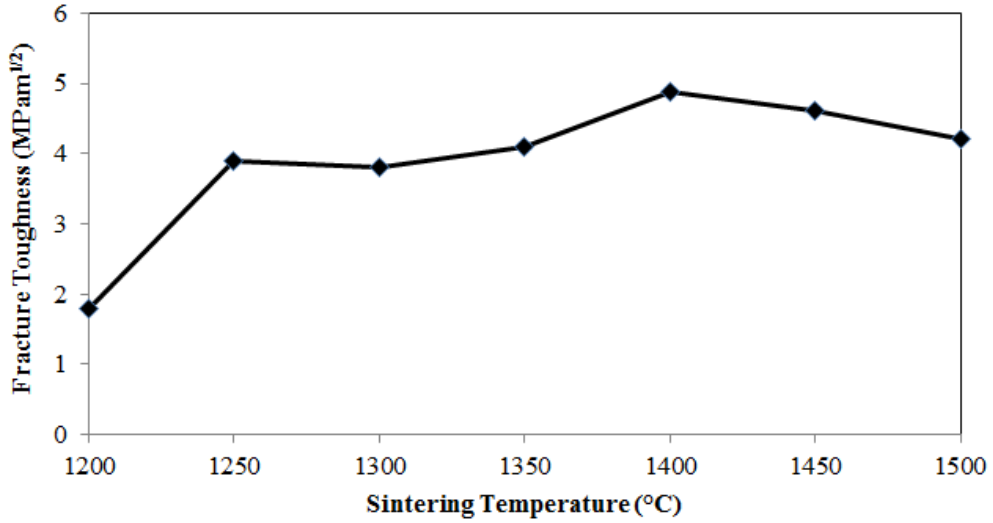

Figure 2.23: Effect of sintering temperature on fracture toughness for sintered forsterite ceramic at various temperature for 2 hours (Tan et al., 2015)

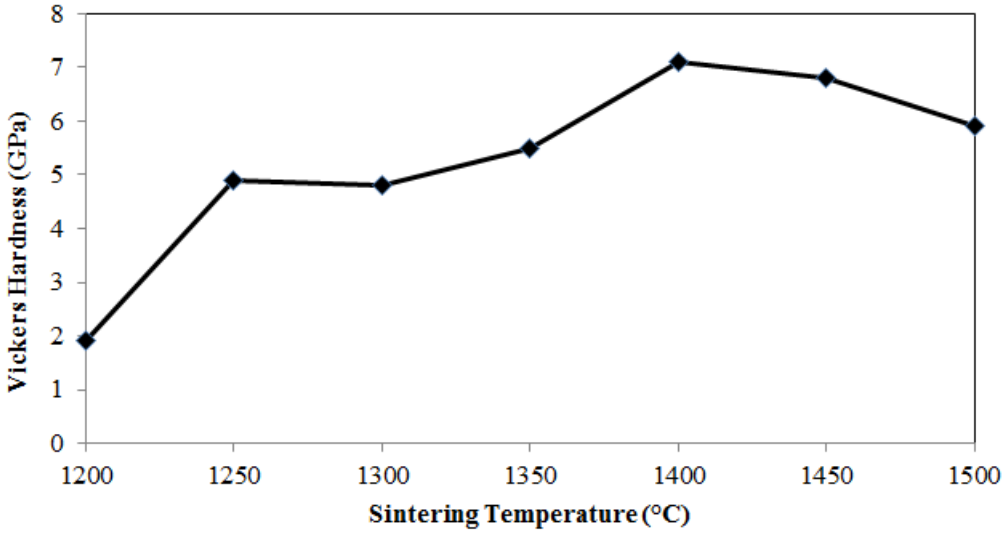

Figure 2.24: Effect of sintering temperature on Vickers hardness for sintered forsterite ceramic at various temperature for 2 hours (Tan et al., 2015)

Figure 2.22 shows that the relative density increased steadily from 70% to 91% as sintering temperature increased from 1200°C to 1500°C. Based on the displayed increasing trend, it can be concurred that increasing the temperature enhanced the densification of forsterite. From Figure 2.23 and Figure 2.24, the results showed both fracture toughness and hardness followed a similar profile where the mechanical properties enhanced from 1200°C to maximum value at 1400°C. The highest Vickers

hardness and fracture toughness of 7.11 GPa and 4.88 $MPam^{1/2}$ were recorded at 1400°C respectively (Tan et al., 2015). Further increment of sintering temperature above 1400°C was found to deteriorate both Vickers hardness and fracture toughness of forsterite.

2.6.3 Two Step Sintering

Investigation regarding two step sintering technique on forsterite powder was performed to overcome the grain growth during the conventional sintering process (Kharaziha & Fathi, 2010). Conventional sintering method, the green compacts are heated in a first cycle at a predetermined rate, and held at a desired temperature until the highest densification level is reached. The grain size increases continuously as density increases which reduces the fracture toughness value. Whereas in the two step sintering methods, green compacts are heated up to a high temperature and held for a short time to reduce the pore sizes in the subcritical scale, then cooled to the lower temperature in order to complete the sintering process.

The forsterite powder was prepared by sol gel method using magnesium nitrate hexahydrate, colloidal silica, polyvinyl alcohol polymer, sucrose and nitric acid as the starting materials. The two step sintering consist of stage 1 where the forsterite ceramic is sintered at T1 with the values between 900°C to 1300°C with step of 50°C at 10°C/min, cooled down at 50°C/min and hold at T2 for 2 hours to 15 hours at temperature of 750°C and 850°C. Finally the samples were cooled down at 10°C/min. The relative density, grain size, fracture toughness and Vickers hardness trends as a function of T1in the second step sintering temperature are shown in Figures 2.25, 2.26, 2.27 and 2.28 respectively.

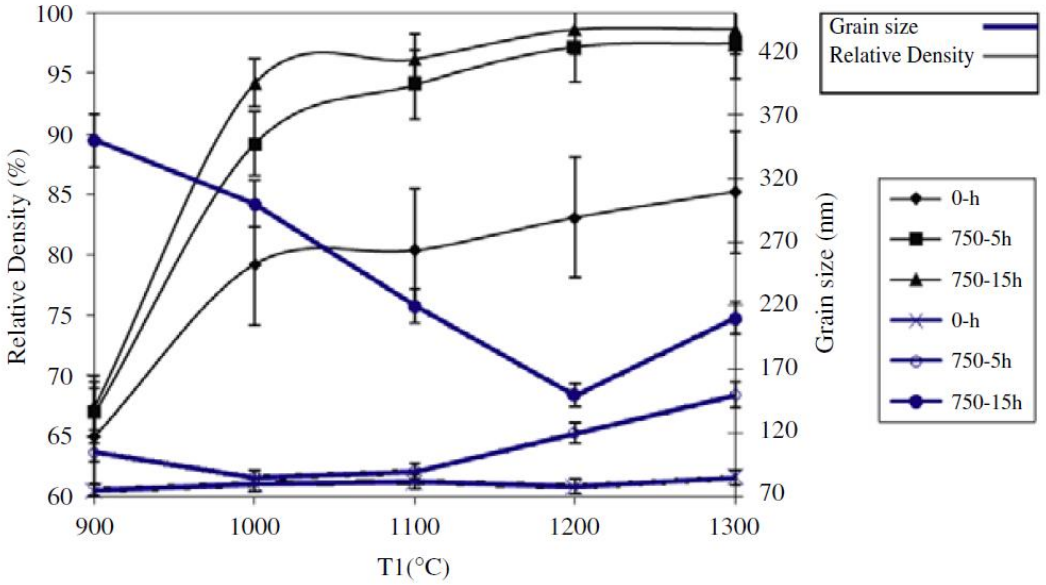

Figure 2.25: Relative density of the sintered samples as a function of *T*1 and grain size after second step temperature at 750°C (Kharaziha & Fathi, 2010)

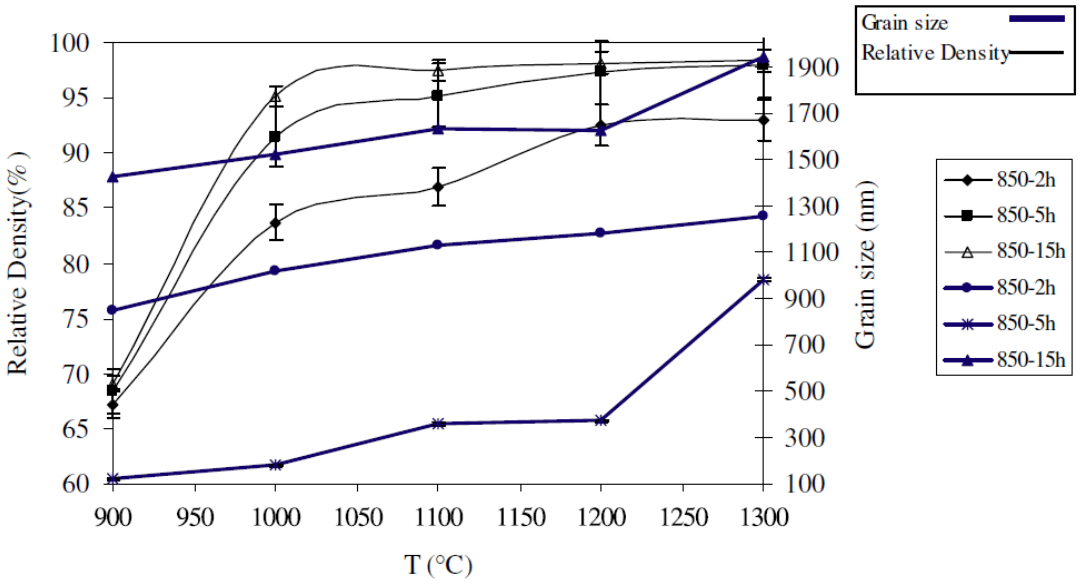

Figure 2.26: Relative density of the sintered samples as a function of *T*1 and grain size after second step temperature at 850°C (Kharaziha & Fathi, 2010)

Figure 2.25 shows significant enhancement in densification of about 79% to 85% for the first step sintering at all temperature range was obtained in the first step of sintering at all temperatures (0h-curve) by increasing the first step temperature up to 1000°C. Figure 2.26 displays a fully dense forsterite ceramic obtained by increasing the dwell time more than 5 hours and second step sintering temperature above 1200°C (*T*1≥

1200°C and a holding time of $T2 \geq 5$). Maximum relative value of 98.6% was recorded after increasing the second step sintering dwell time from 2 hours to 15 hours. Previous study suggested grain boundary diffusion needs to remain active, while the grain boundary migration is suppressed to achieve densification without significant grain growth (Wang et al., 2006). Triple point drag is a mechanism to deter grain boundary movement. The strife between boundary mobility and junction mobility are related to grain growth. The drag takes place when the junctions are in static condition at low temperature eliminating the competition between the junctions. The T2 value of 850°C maybe not low enough to achieve the static condition. The optimal condition to produce forsterite powder using the two step sintering technique are 1200°C and 750°C for the first step and second step sintering temperatures respectively with 5 hours dwell time for second step sintering only. Pores were evident between grains when the first step sintering temperatures were lower than 1200°C and second step sintering temperature set at 750°C.

As per Figure 2.27 and 2.28, the fracture toughness improved from 1.10 ± 0.5 $MPam^{1/2}$ (at $T1$ = 900°C) to 43 ± 0:3 $MPam^{1/2}$ (at $T1$ = 1200°C). Hardness was improved from 520 ± 45 Hv (at $T1$ = 900°C) to 980 ± 20 Hv (at $T1$ = 1200°C) for the prolonged soaking at 750°C up to 5 hours.

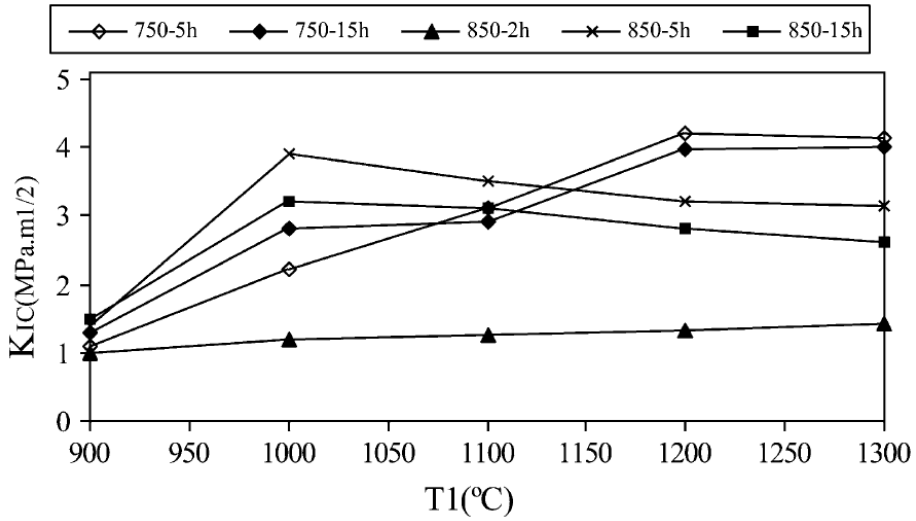

Figure 2.27: Fracture toughness of forsterite bulk as a function of *T*1 after second step temperatures at 750°C & 850°C (Kharaziha & Fathi, 2010)

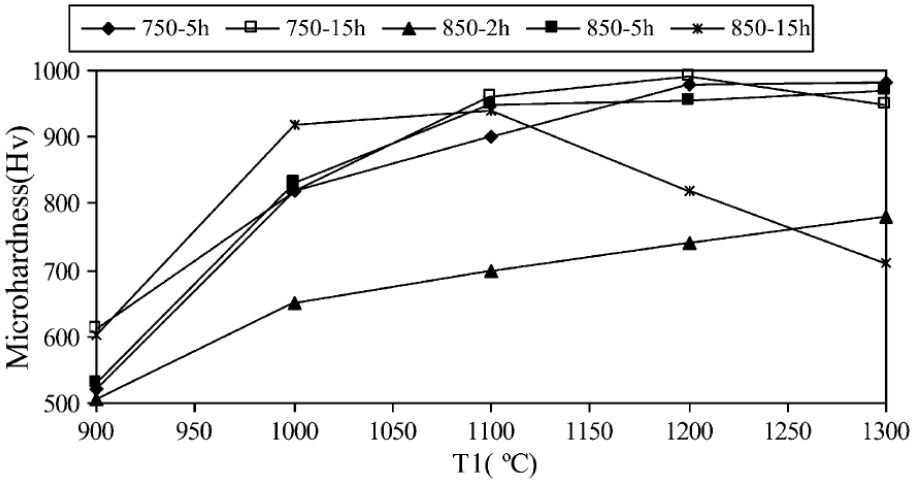

Figure 2.28: Vickers microhardness of forsterite bulk as a function of *T*1 after second step temperatures at 750°C & 850°C (Kharaziha & Fathi, 2010)

High hardness and fracture toughness of 955 ± 15 Hv and 3.2 ± 0.25 $MPam^{1/2}$, respectively was recorded at (*T*1 = 1200°C and *T*2 = 850°C) with a prolonged soaking at 850°C up to 5 hours. Prolonged soaking at 850°C up to 15 hours resulted in decline in hardness and fracture toughness. Prolonged soaking of up to 5 hours at (*T*1 = 1200°C and *T*2 = 750°C), provided higher value in hardness and fracture toughness respectively.

Similar two step sintering process was performed using forsterite powder prepared by mechanical activation recorded lower fracture toughness, hardness value and grain size of 3.61 ± 0.1 $MPam^{1/2}$, 940 ± 10 Hv and 60 nm to 75 nm respectively at ($T1$ = 1300°C and $T2$ = 750°C) with a prolonged soaking at 750°C up to 15 hours (Fathi & Kharaziha, 2009b). The relative density results obtained by two step sintering method are higher than previous results obtained by conventional pressureless sintering method (Mazaheri et al., 2007; Han et al., 2007). Nonetheless, there are previous studies that show increasing grain growth indicating two step sintering method is able to regulate grain growth depending on several factors including the starting precursors used to prepare the forsterite powder (Ghosh et al., 2007; Yu et al., 2007).

In summary, this chapter provided an overview of the various parameters that control the sinterability of forsterite ceramics. The selection of starting precursors to prepare the forsterite powder is an important factor which influences the mechanical properties. Heat treatment temperature, sintering temperature has direct relationship with densification. However over firing will result in declining mechanical properties. Secondary phase may not be entirely eliminated with extensive duration of heat treatment and sintering dwell time. Prolonged ball milling duration does not necessarily provide improved mechanical properties. Therefore, these parameters should be further optimized for improved mechanical properties of forsterite ceramic via conventional presureless sintering.